ISSN: 2096-3246
Volume 54, Issue 02, October, 2022

AN ANALYTICAL STUDY ON DETERMINING THE FUNCTIONAL POTENTIALITY OF NON MOMENT RESISTING BRACED FRAMES TO MINIMIZE EARTHQUAKE INDUCED DAMAGE

K Raghu
SJCIT Chickballapur, rksjcit@gmail.com

Sathish Kumar S R
IIT Madras, kim@iitm.ac.in

G Narayana
SJCIT Chickballapur, narayanagsjcit@gmail.com

Abstract: In this research article, an analytical study on determining the functional potentiality of non moment resisting braced frames to minimize earthquake induced damage has been presented. A self-centering damage avoidance idea called a Resilient Slip Friction Joint (RSFJ) was created for steel Moment Resisting Frames employing a unique Resilient Slip Friction Joint (RSFJ). The RSFJs make it possible for a gap to open up in the connection during loading, and they re-center the system when loading has been completed. An analytical model was constructed in order to precisely anticipate the behaviour of this system in terms of its moment-rotation relationship. A single-bay ten-storey concentric braced frame with diagonal Non-Buckling bracing is chosen for studying their effect during earthquake loadings. This study aims to analytically obtain the seismic performance of non-moment resisting braced frames with and without RSFJ dampers. The frames were modelled and designed in ETabs software and a pushover analysis & time history analysis was performed.
Keywords: Resilient Slip Friction Joint, Dampers, Non-Moment resisting braced frames, Moment resisting braced frames, Earthquake, Damage

1. Introduction

Buildings sway back and forth with amplitude proportionate to the energy fed in when there is severe ground shaking. The earthquake response can be greatly enhanced if a large percentage of this energy is spent during building motion. The level of damage is determined by how this energy is spent in the structure.

The major responsibility of a structural engineer is to ensure public confidence in the built environment's safety. It is not only essential to create structures that provide safe and reliable shelter for people, but it is also the engineer's goal to achieve economy, architectural appeal, and structural performance through the design process. There is also the added problem of constructing structures that can withstand and weather such major natural disasters in seismically high-risk areas.

The approach to developing earthquake-resistant structures in the field of structural engineering has changed dramatically during the last several decades. While the primary goal of seismic codes has always been and will continue to be to prevent unexpected collapse and failure of structures during

significant events, the need for more optimal and efficient solutions has become increasingly apparent in recent years.

The term "performance-based design" refers to a method in which design criteria are based on achieving particular performance targets under different levels of seismic hazard. The lateral floor displacements, peak floor accelerations, or a target damage state of the building as a result of an earthquake are examples of performance targets.

Although the performance-based design and its adoption in modpracticetise has proven useful and enabled increased reliability of expected structural performance of buildings during seismic events, the ever-increasing demand for optimizing structural performance to minimize economic loss, and repair costs will continue to push engineers to come up with better solutions.

High-performance structural systems that can resist intense ground shaking with little or no structural damage (outside of replaceable energy dissipation parts) are needed to lessen the economic disruption caused by earthquakes and to develop more resilient, sustainable cities. A novel class of seismic lateral force resisting systems has been created to address this need.

These damage-resistant systems soften the structural response by elastic gap opening mechanisms rather than yielding in core structural parts, reducing or preventing structural damage to non-replaceable elements. Friction elements or changeable yielding energy dissipation components are also included to dissipate seismic energy.

The main issue for structural engineers when developing earthquake-resistant structures is to create systems that are both ductile and stiff. The traditional lateral force resisting systems, such as the moment-resisting frame (MRF) and the concentrically braced frame (CBF), has been in use for many years but only provide mediocre results.

Engineers were inspired to focus significant research attention on the development of new lateral resisting systems with more stable hysteretic behavior, adequate ductility, damage control, and the energy dissipating capacity due to the lack of stiffness of a moment-resisting frame and the limited ductility of a concentrically braced frame. Fortunately, several recent breakthroughs have brought engineers closer to building more efficient earthquake-resistant structures.

Following the earthquakes in Northridge, California, in 1994, and Kobe, Japan, some studies have shifted their focus to a seismic design strategy that allows for the full integration of passive damping devices, also known as energy dissipation systems, into the brace component. Passive energy dissipation devices include viscous fluid, electromagnetic, viscoelastic, and metallic yield, as well as frictional dampers.

In comparison to other types of passive dampers, friction dampers provide stable energy dissipation due to simple friction mechanisms created on the sliding shear surfaces. During a variety of cyclic loads, their hysteretic behaviors are maintained with consistent slip resistance. During a variety of cyclic loads, their hysteretic behaviors are maintained with consistent slip resistance. Slip resistance loads can be easily controlled by measuring bolt pretension or changing surface conditions

As a result of their simple mechanism, ease of manufacturing, and long-term maintenance, friction dampers have become widely used in the practical building industry for earthquake design. The use of these damper devices on the brace member contributes significantly to the protection of key

structural members against severe damage. Traditional seismic load resistance systems, such as moment resisting frames (MRFs) and concentrically braced frames (CBFs), frequently disperse seismic energy by causing ductile inelastic deformation in specified structural parts. In high seismic zones, where costly repairs are frequently necessary after moderate earthquakes, such a seismic design technique may not be acceptable from a life-cycle cost standpoint.

In designing efficient earthquake-resistant steel structures there are two overarching performance objectives: (1) adequate lateral stiffness to restrict large shifts during elastic range to minor and moderate earthquakes, and (2) sufficient ductility to withstand large inelastic displacements under extreme earthquakes and prevent sudden collapse. The balance of these two factors, stiffness and ductility, is the key to maximizing the seismic performance of structures.

Earthquake based damages are usually caused by the following forces:

Due to the inertia of the masses, as the base of a building moves, the superstructure, including its contents, shakes and vibrates in a very irregular manner from its resting position. When the structure's base moves to the right, the building moves to the left about the base, as though pulled to the left by an unseen force known as Inertia Force.

There is no force at all, but the building's mass prevents it from moving. During an earthquake, the ground moves in three mutually perpendicular directions at the same time, making the process much more complicated.

Seismic Load: The force F represents the resultant lateral force or seismic load. The dead, living, snow, wind, and impact loads are all unique from the force F. The effect of horizontal ground motion on the building is similar to that of a horizontal force operating on the structure, hence the term Seismic Load. The performance-based seismic design process assesses how a structure will behave in the event of a possible hazard. It also takes into account the uncertainties that come with quantifying possible hazards and assessing the actual building response. Identifying and measuring a building's performance capability is an important aspect of the performance-based design process. The selection of design requirements expressed in the form of one or more performance objectives is the first step in performance-based design. Each performance goal specifies the acceptable risk of sustaining certain levels of damage. At a given level of seismic danger, the consequential losses that arise as a result of damage are estimated. Losses can be caused by structural, nonstructural, or both types of deterioration.

They can be measured in terms of fatalities, direct economic expenditures, and downtime (time spent out of service) as a result of damage. Identifying and measuring a building's performance capability is an important aspect of the design process in performance-based design, as it guides the many design decisions that must be made.

It is an iterative process that begins with the selection of performance objectives, then moves on to the creation of a preliminary design, an assessment of whether the design meets the performance objectives, and finally, if necessary, redesign and reassessment until the desired performance level is reached.

The selection of performance targets is the initial element in PBSD, and it is made up of two parts: a performance level and a hazard level that describes the predicted seismic load at the site. The

performance based design process is depicted in the figure 1.

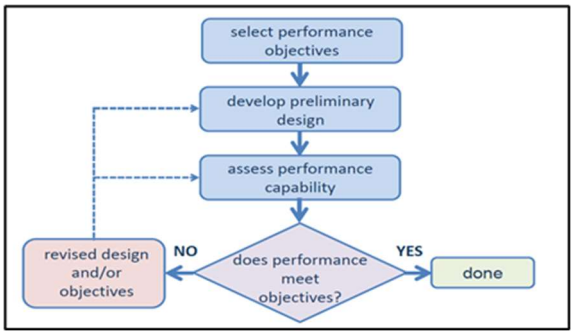

Fig. 1 Performance based design process

2. Review of Literature

According to Canxing Qiu, Jiawang Liu, Jun Teng (2021), the superelastic strain of SMAs has an upper limit, beyond which the material completes the austenite to martensite phase transformation and is followed by noticeable strain hardening. The strain hardening behavior would not only induce high force demand to the protected structures, but also cause unrecoverable deformation. More importantly, the SMAs may fracture if the deformation demand exceeds their capacity under severe earthquakes. In the case of installing SMA braces (SMABs) in the multi-story concentrically braced frames (CBFs), the material failure would lead to the malfunction of SMABs and this further causes building collapse. The friction mechanism could behave as a "fuse" through capping the strength demand at a constant level. The proposed study attempts to reduce these risks. Comparative results show the SMAFDB is superior to the counterparts. Under the FOE and DBE ground motions, the SMAFDBs successfully eliminated residual deformations as the SMABs do, and achieved identical maximum interstory drift as the FDBs. Under the MCE ground motions, the SMAFDBs not only well addressed the brace failure problem that was possibly encountered in the SMABs, but also better controlled residual deformation than the FDBs.

Francesca Barbagallo, Melina Bosco, Edoardo M.Marino, Pier Paolo Rossi (2021) investigates the seismic performance and the cost of case-study buildings embedding different braced steel structures, namely concentrically braced frames, eccentrically braced frames with short or long links, braced frames with buckling restrained braces or double-stage yield buckling restrained braces and dual systems consisting of braced frames with buckling restrained braces and moment-resisting frames with semi-rigid connections. Lihua Zhu and Cheng Zhao (2020) explored that the structural details and seismic behaviors of the self-centering systems proposed in recent years, including connections, energy dissipating braces, and steel frames, are condensed in categories. Canxing Qiu & Songye Zhu (2020) presented a new strategy to enhance the seismic performance of self-centering concentrically braced frames (SCCBFs). A hybrid strategy, which combines a SCCBF with a moment-resisting frame or buckling-restrained-braced frame, is first investigated, which show evident reduction in peak deformation demands. Pei Chi, Wenlong Tian, Tong Guo, Dafu Cao, and Jun Dong (2019) presented a parametric study on the seismic response of intermediate and high-rise steel-framed buildings (9- and 16-story steel-framed buildings) with novel self-centering tension-only braces (SC-

TOBs). Amir Kari, Mehdi Ghassemieh, Baitollah Badarloo (2019) proposed a robust self-centering energy-dissipative brace to be used in structural frames. The brace is capable of providing adequate energy dissipation capacity in the structure while simultaneously bringing the structure to its original configuration after the earthquake. The proposed model is developed as a better alternative to buckling-restrained brace efficacy. Can-Xing and Qiuab Songye Zhu (2017) proposed a performance-based seismic design (PBSD) method for steel braced frames with novel self-centering (SC) braces that utilize shape memory alloys (SMA) as a kernel component. Superelastic SMA cables can completely recover deformation upon unloading, dissipate energy without residual deformation, and provide SC capability to the frames. The presented PBSD method is essentially a modified version of the performance-based plastic design with extra consideration of some special features of SMA-based braced frames (SMABFs). A. Deylami and M. A. Mahdavipour (2016) observed that the residual deformations are more sensitive to degradation than maximum deformations. C. Christopoulos; R. Tremblay; H.-J. Kim; and M. Lacerte (2008) presented a new bracing system that can undergo large axial deformations without structural damage while providing stable energy dissipation capacity and a restoring force has recently been developed. The proposed bracing member exhibits a repeatable flag-shaped hysteretic response with full recentering capabilities, therefore eliminating residual deformations.

3. Self-Centering Friction Damping Braces

To efficiently bear the lateral load conveyed by seismic activity, the SFDB may be used in conjunction with other brace systems. The SFDBs' specifics are just a rough sketch. They are made up of two shear plates, four shear bolts, slotted bolt holes, and super-elastic SMA stranded wires that are looped around the fixed anchors to provide strength and durability. Through the application of direct shear pressures operating in accordance with the longitudinal direction of slotted bolt holes, the shear plates may be moved. The shear friction mechanism, which produces steady energy dissipation, has a considerable impact on the roughness conditions between shear faying surfaces and the normal force, which is defined by the length of the bolt adjustment bolt. It is only possible to use the super-elastic SMA-stranded wires to withstand external excitation under tension, and they are primarily responsible for providing the recentering capacity to the SFDB system.

The response of numerical single-degree-of-freedom (SDOF) spring models under a variety of seismic stresses were used to assess the seismic performance and evaluate the SFDB systems constructed with parametric features. As a consequence of these numerical analytical findings, this research also presents the performance-based optimum design approaches for the SFDB system, which serves as an example of a smart self-centering device of this kind. Modeling the response mechanisms, which are composed of both recentering behavior and slip friction, as appropriate SDOF component springs calibrated to experimental test findings and idealized by the stiffness models often employed in numerical simulation is done. When these component springs are simulated with varied prototype scale parameters, nonlinear time-history studies are performed to mimic the various hysteresis curves seen in the experiments. For the nonlinear time-history studies, two sets of ground motion data records (i.e., 20 basic design earthquake (BDE) records and 20 maximum considered earthquake (MCE) records) are chosen for consideration. With the help of the

study findings, it will be possible to confirm that recentering capability corresponds with energy dissipation capacity in the SFDB system.

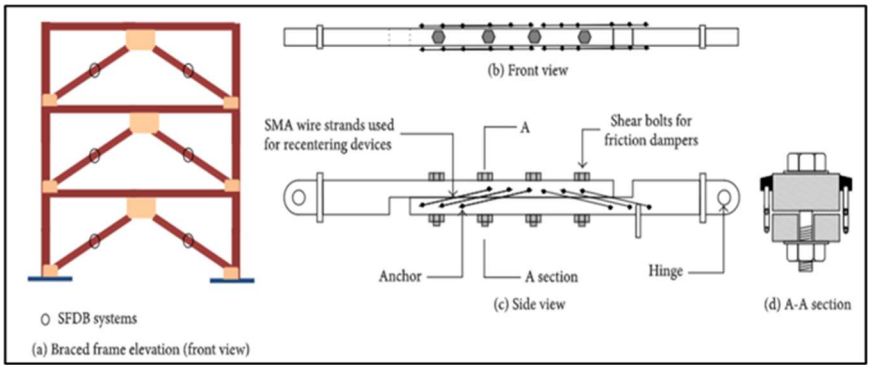

Fig 2: Self centering friction damping braces

SFDB models are composed of two component springs, which correspond to super-elastic SMA stranded wires and friction damper systems, respectively in the analytical form. These component springs were constructed in sequence to model the behavior of the SFDB, with consideration given to how each component mechanism interacted with the others during force transmission and the interaction between them.

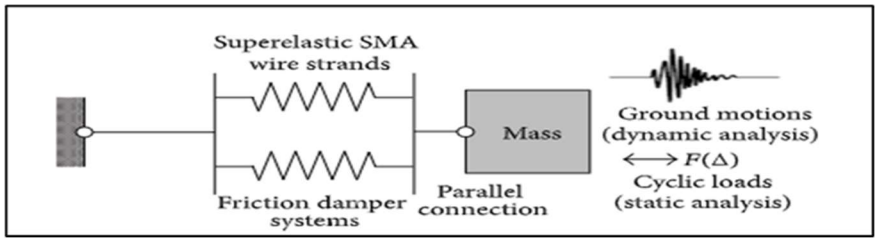

Fig 3. Component spring model

Friction and the super-elastic nickel-titanium shape memory alloy wires, which are employed to perform the self-centering action, are responsible for the dissipation of energy. By repeatedly loading the brace to failure on a small scale, a prototype SFDB was developed, manufactured, and tested. When an elastic spring (such as post-tensioned cables or pre-pressed springs) is combined with a damping mechanism (such as friction, yielding, or viscous) the result is a flag-shaped reaction, which is well-documented. On the other hand, if one wants to get a flag-shape response with zero secondary stiffness (1=0), the standard approaches seem to be useless.

4. Resilient Slip Friction Joint (RSFJ)

4.1 FRICTION-DAMPED BRACED FRAMES

From a logical standpoint, it seems desirable to locate an alternate source of energy dissipation to safeguard the primary structural parts from damage. The friction brake is, without a question, the most extensively used way of extracting kinetic energy from a moving body out of all the options that are accessible. Several static and dynamic tests on various faying surface treatments were carried

out under repeated reversals of loads under controlled conditions.

Slip joint hysteresis loops are fastened together by high tension 1/2 in. (12.7mm) diameter high strength bolts to form a single unit (ASTM A325). The greatest results were obtained using a heavy-duty brake lining pad, which was put between the sliding steel surfaces and was the most expensive. A dependable and reproducible performance has been achieved; in addition, the hysteresis loops have a rectangular shape with little fading even after many more cycles of reversals than are seen in subsequent earthquakes. Much bigger amounts of energy can be disposed of by friction than can be disposed of using any technique that requires a harmful process of yielding materials. Instead of breaking, vibrating buildings use braking to slow down their motion, which is similar to how vehicles do it.

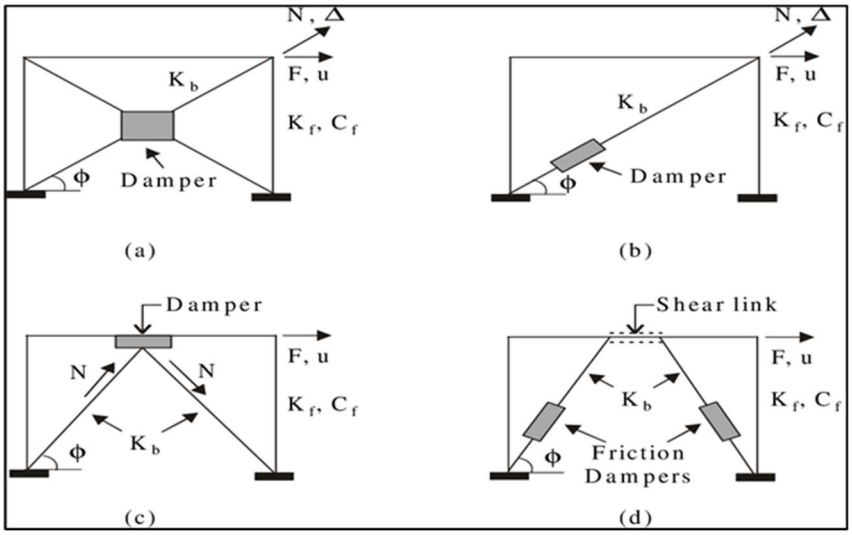

Fig 4. Friction damped braced frames

Each bracing in the moment-resistant frame of the proposed structural system is equipped with a friction device, which reduces the friction between the bracings. Under regular service loads and mild earthquakes, the device is not intended to slide or malfunction. If the frame is subjected to significant seismic excitations, the device slips at a specified load before the other structural parts of the frame begin to fail. After then, slippage in the gadget serves as a mechanism for the disposal of energy via friction. Because the braces are carrying a constant load, the moment is responsible for carrying the remaining weights.

4.2 BRACE WITH FRICTION DEVICE

Using a friction joint with slotted holes, you may slide in both tension and compression. However, you must ensure that the brace is constructed such that it does not buckle in compression up to the slip load value. Also possible are friction joints that slide while under a high load in tension, as well as when under a low load-in compression, before the brace buckling. In most cases, the bracing is relatively thin and is intended to be effective only in tension. As a result, the friction joint slides when the weight is applied in tension but does not slip back when the load is removed. The brace will not slide again until it has been extended beyond the last expanded length, resulting in very low energy waste during the succeeding cycle.

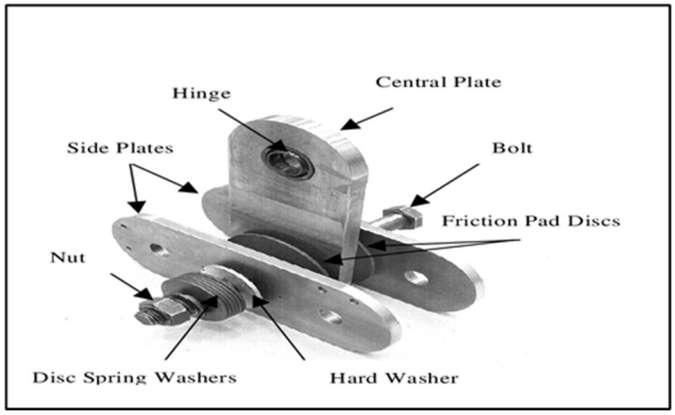

Fig. 5 Brace with a friction device

5. DESIGN EXAMPLE

5.1 DESCRIPTION OF THE STEEL BRACED FRAME

The frame under consideration is a 10 storied steel braced frame. The steel frame is 37 m long and 6.1 m wide as shown in Fig. 6. The stiffness of the members of the frame was adjusted to suite the earthquake input used in this study. The properties of beams and columns that were used are given in Table 1 In the present study, Non-Moment Resisting Braced Frame (NMRBF) were considered for the analysis. A non-moment resisting braced frame (NMRBF) with concentric Non-Buckling bracings in all storeys, wherein the lateral load is resisted by bracings alone

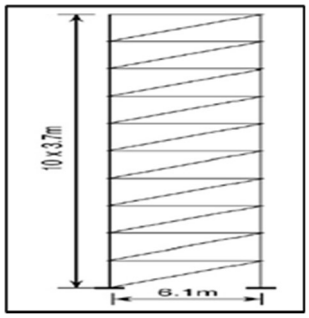

Fig. 6 Storeys and in which the lateral load is resisted only by the bracings

Floor Level	**Beam**	**Column**	**Bracings**
	Area (mm2)	Area (mm2)	Area (mm2)
Story10	9230	6130	770
Story 9	9230	6130	770
Story 8	9230	8500	770
Story 7	9230	8500	1020
Story 6	9230	12120	1020
Story 5	11070	12120	1020

Story 4	11070	18490	1510
Story 3	11070	18490	1510
Story 2	11070	39010	1510
Story 1	11070	39010	1510

Table 1. Member properties

ii) General structural information:

Table 2. Structural and site aspects of steel frames

Structural Parameters	**MRBF**	**NMRBF**
No of storey's	10	10
Height of each storey (m)	3.7	3.7
Width (m)	6.1	6.1
Site Parameters	**MRBF**	**NMRBF**
Zone factor (Z)	0.36	0.36
Importance factor (I)	1.2	1.2
Response reduction factor (R)	5	5
Type of soil	Medium	Medium
Material properties	**NMRBF**	**MRBF**
Grade of steel	FE 250	FE 250
Yield strength(N/mm^2)	250	250
Expected yield strength (N/mm^2)	275	275

The numerical modelling and analysis of conceptual steel non-moment resisting braced frame(NMRBF) equipped with RSFJs are modelled by using ETABS software. The flag-shaped hysteresis of the RSFJ can be modelled using conventional ETABS software though properly calibrating the design parameters.

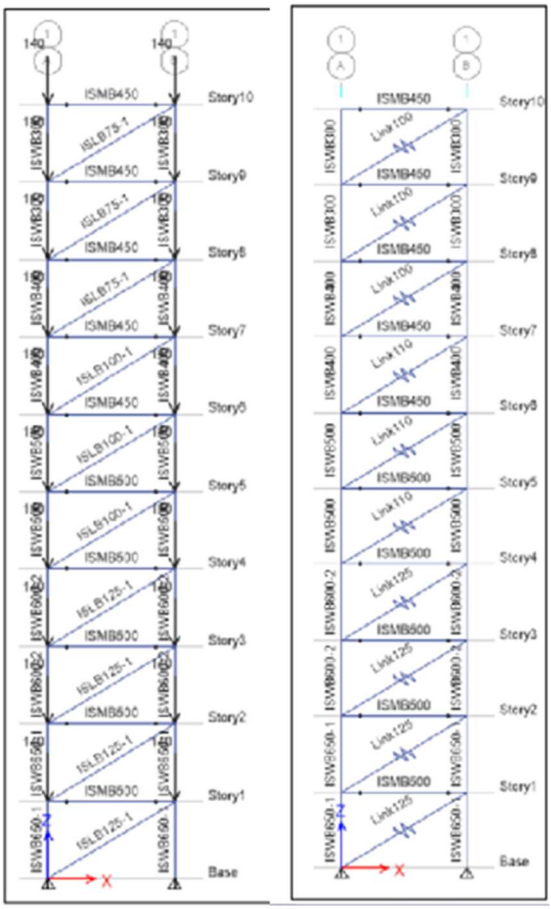

Fig. 7 Non moment resisting braced frame(NMRBF) with and without damper

6. Result Analysis

The design force for each of the structural components in this example is derived by using the Equivalent Static Approach (ESM), which is a Forced-Based Design (FBD) method and is detailed in (IS1893-2016). The Modal Response Spectrum Analysis Method, often known as RSA, would have worked just as well.

Table 3 Results of linear static analysis

Floor Level	**Section**	**Axial Stiffness (kN/mm)**	**Fult (kN)**
Story 10	ISLB75	22	33.50
Story 9	ISLB75	22	58.43
Story 8	ISLB75	22	76.79
Story 7	ISLB100	29	98.06
Story 6	ISLB100	29	106.7

Story 5	ISLB100	29	106.5
Story 4	ISLB125	42.5	127.6
Story 3	ISLB125	42.5	123.7
Story 2	ISLB125	42.5	124.7
Story 1	ISLB125	42.5	132.4

Table 4. Initial configuration of RSFJ braces for Non moment resisting braced frame(NMRBF)

Story	**Brace Code**	**Section**	**Initial Stiffness (kN/mm)**	**F_{slip} (kN)**	**F_{ult} loading (kN)**	**F_{ult} unloading (kN)**	**$F_{resudial}$ (kN)**	**Δmax (mm)**
Story 10	RSFJ 35	ISLB 75	22	17.5	35	45	25	80
Story 9	RSFJ 60	ISLB 75	22	30	60	20	12	80
Story 8	RSFJ 80	ISLB 75	22	40	80	34	18	80
Story 7	RSFJ 100	ISLB 100	29	50	100	41	21	80
Story 6	RSFJ 100	ISLB 100	29	62.5	100	41	21	80
Story 5	RSFJ 100	ISLB 100	29	62.5	100	41	21	80
Story 4	RSFJ 125	ISLB 125	42.5	75	125	58	29.5	80
Story 3	RSFJ 125	ISLB 125	42.5	75	125	58	29.5	80
Story 2	RSFJ 125	ISLB 125	42.5	75	125	58	29.5	80
Story 1	RSFJ 150	ISLB 125	42.5	75	150	45	25	80

6.1 PUSHOVER ANALYSIS

The upper bound limit for the buildings susceptible to ULS earthquakes according to the New Zealand standard is 2.5 percent. Additionally, it implies that in the event of an MCE event (with a 1/2500 yearly period of exceedance), this limit may be raised to 3.75 percent.

6.1.1. Non moment resisting braced frame (NMRBF) without dampers

i) Pushover curve

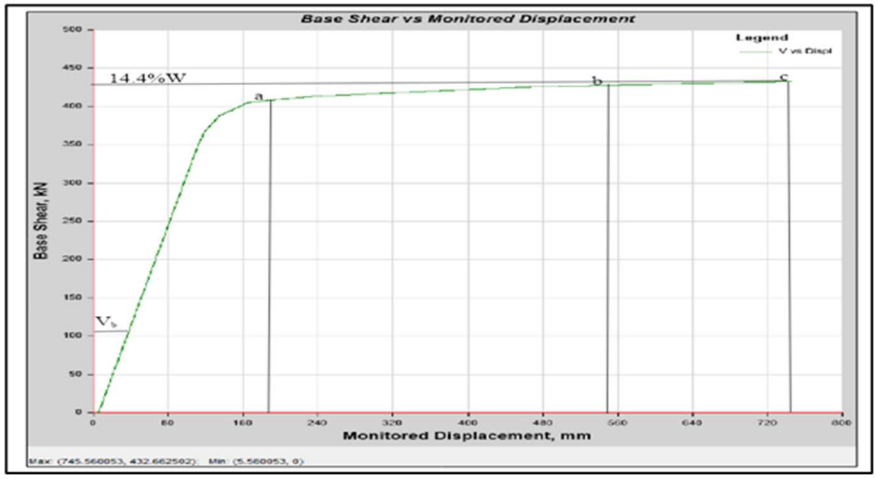

Fig 8. Monitored displacement v/s base shear for Moment resisting braced frame with dampers.

The maximum node displacement amounts to 0.745 meters, which is equivalent to a percentage H value of 2%. The Pushover Curve demonstrates that the structure has a Base Shear Capacity that is much higher than the Design Base Shear. On the curve, the points a, b, and c that correspond to 0.5 percent, 1.5 percent, and 2 percent of Displacement correspondingly are indicated. The proportion of the building's seismic weight that is devoted to its base shear capacity is roughly 14.4 percent.

ii) Hinge status

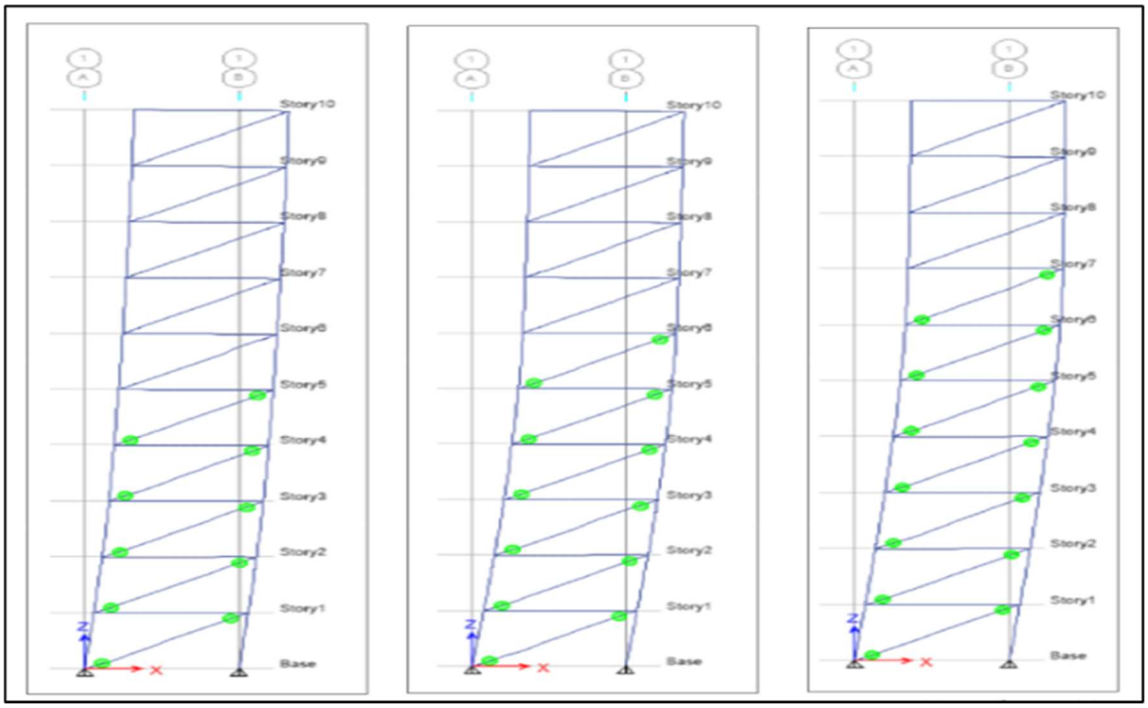

Fig. 9 Formation of Hinges in the frame at point ‘a’, ’b’ and ’c’ respectively

The formation of hinges for earthquakes for a 10-story structure is shown in fig 9 above. To assess hinge development, the frame at points are a, b, and c. It is visible that the hinges begin to develop at frame at point ‘a’, ‘b’, and ’c’ although they are quite safe and do not pose any hazard problems.

ISSN: 2096-3246
Volume 54, Issue 02, October, 2022

6.2 Non moment resisting braced frame (NMRBF) with dampers

i) Pushover curve

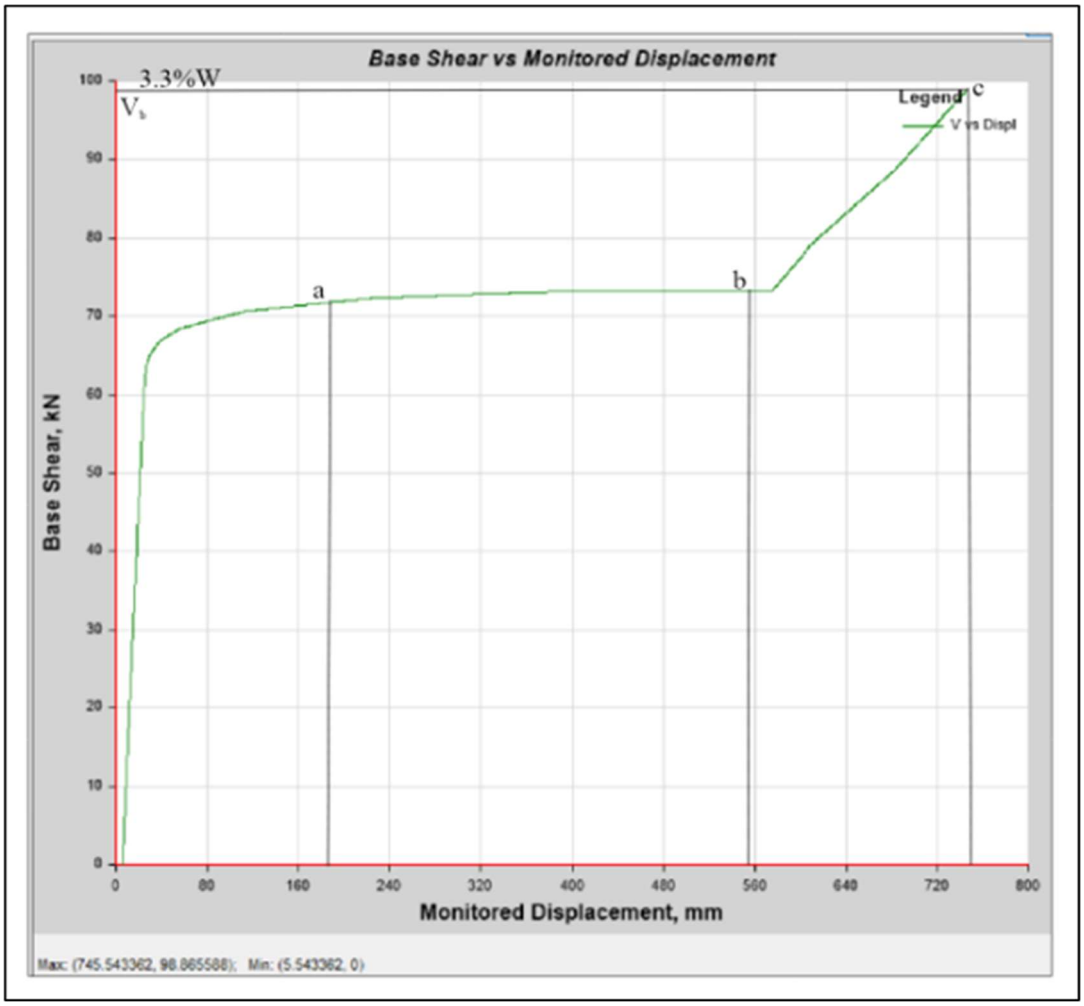

Fig 10 Monitored displacement v/s base shear for Non Moment Resisting Braced frame with dampers

The maximum node displacement amounts to 0.745 metres, which is equivalent to a percentage H value of 2%. Based on the Pushover Curve, it can be shown that the building has a Base Shear Capacity that is much lower than the Design Base Shear. On the curve, the points a, b, and c have been labelled to correspond to 0.5 percent, 1.5 percent, and 2 percent of Displacement, respectively. The proportion of the building's seismic weight that is devoted to its base shear capacity is roughly 3.3%.

ii) Hinge status

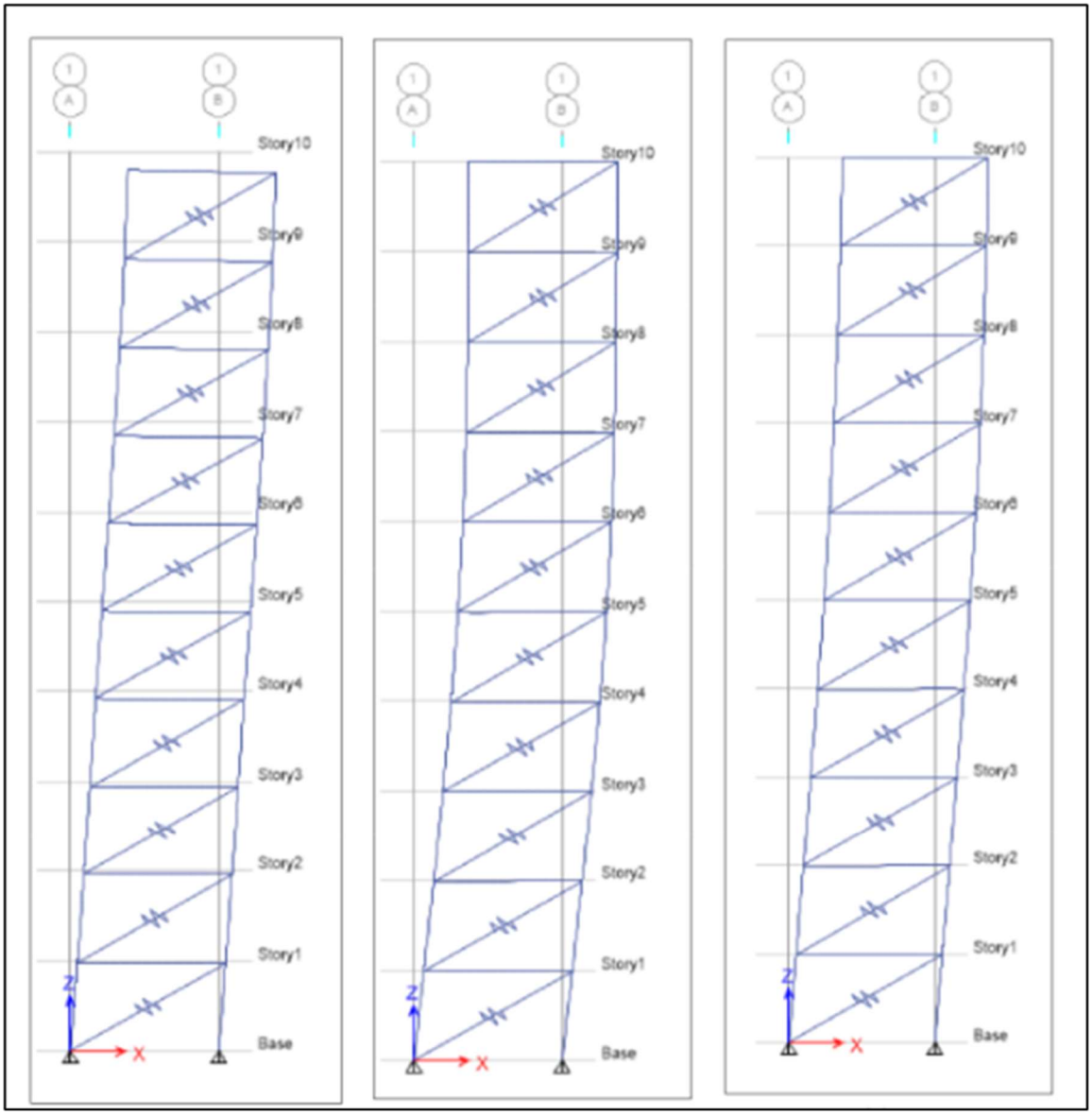

Fig. 11 No formation of Hinges in the frame at points ‘a’, ’b’ & ’c’ respectively

The pushover study reveals that the NMBRF with dampers is functioning. This conclusion may be drawn from the data.

6.2 Nonlinear time history analysis

6.2 Non Moment Resisting Braced Frame (NMRBF) with Dampers

6.2.1 Hinge status

i) Altadena - Eaton Canyon Park Earthquake

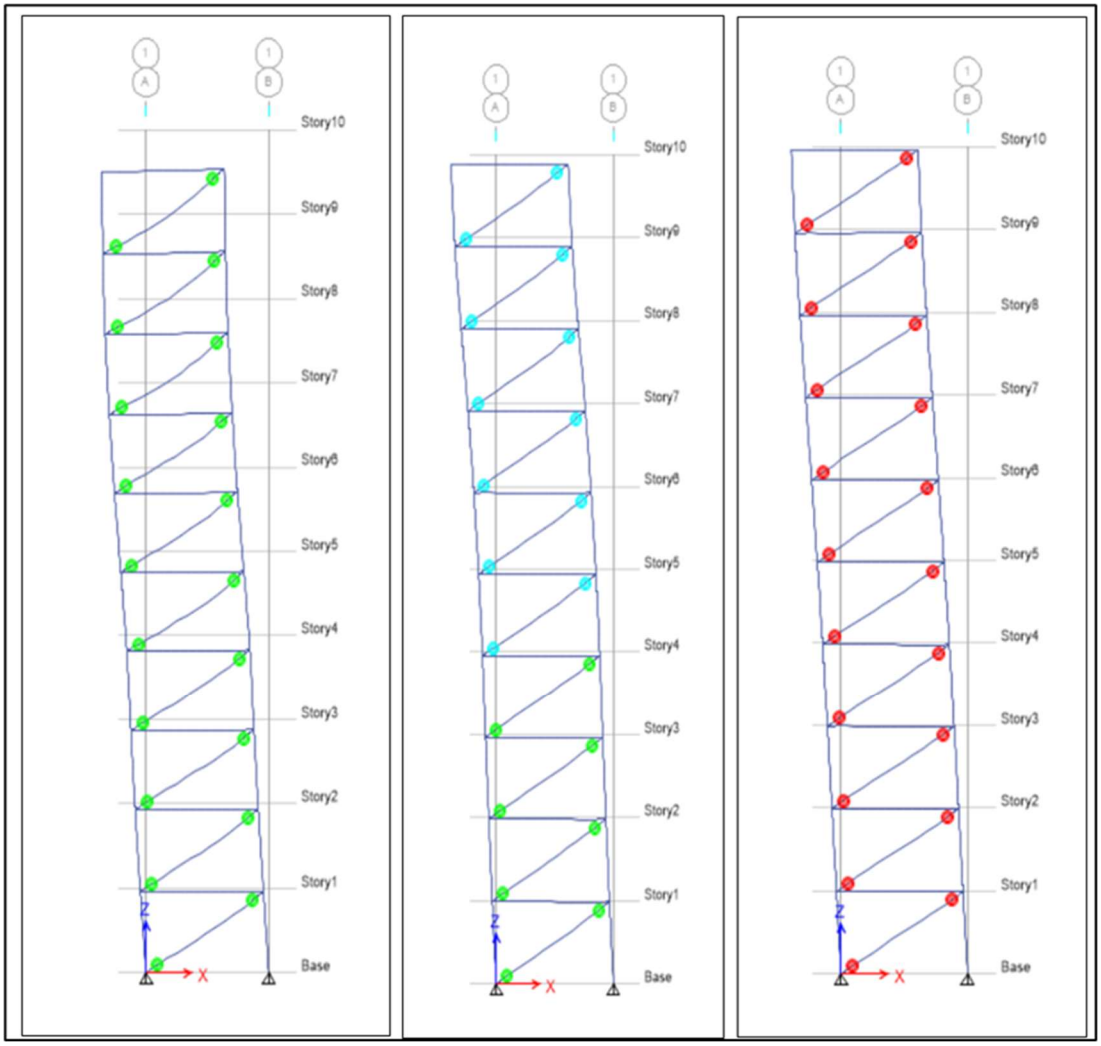

Fig. 12 Formation of hinges at 2.2 sec, 4 sec and 15sec displacement for Altadena - Eaton Canyon earthquake.

The formation of hinges for Altadena - Eaton Canyon Park earthquake for a 10-story structure is shown in fig. 12 above. To assess hinge development, the three time intervals are 2.2 seconds, 4 seconds, and 15 seconds. It is visible that the hinges begin to develop at 2.2 seconds, although they are quite safe and do not pose any hazard problems. The 10 story skyscraper's 4 levels are secure while the hinges were still inclined for 4 seconds, but the structure is likely in danger above those stories. The structure began to tilt significantly from its initial position after 4 seconds, and the hinge assembly is now in a dangerous scenario.

ii) EL Centro Array Earthquake

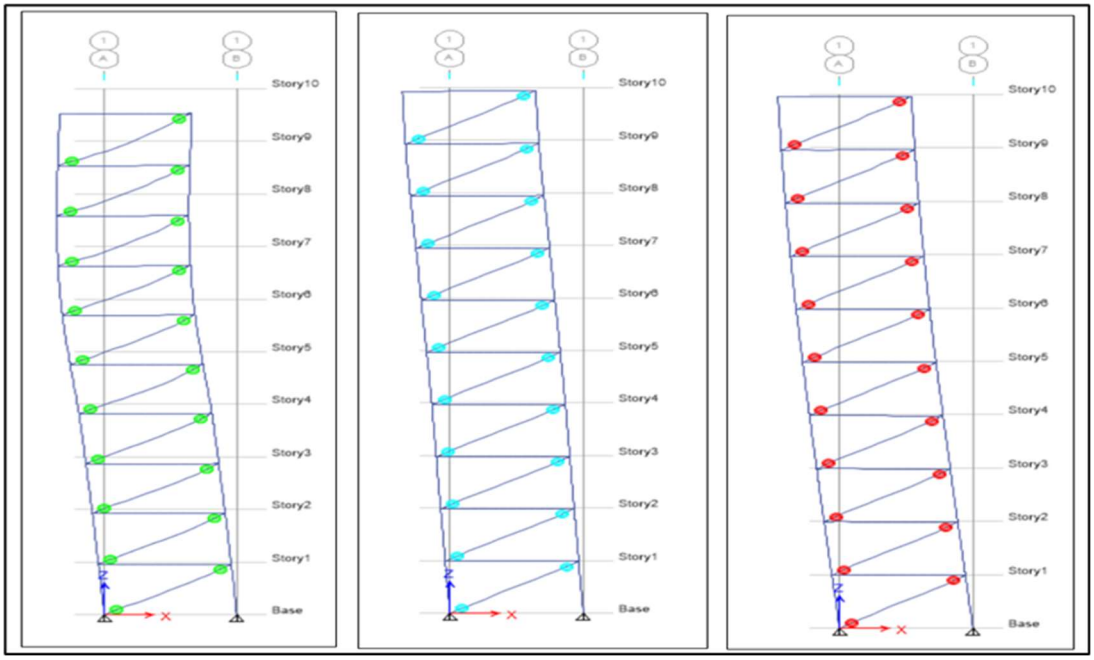

Fig. 13 Formation of hinges at 6sec, 7.4sec and 15sec displacement for EL Centro Array earthquake.

The formation of hinges for EL Centro Array 6 earthquake for a 10-story structure is shown in fig. 13 above. To assess hinge development, the three time intervals are 6 seconds, 7.4 seconds, and 15 seconds. It is visible that the hinges begin to develop at 6 seconds, although they are quite safe and do not pose any hazard problems. The hinges on the entire level of the 10-story skyscraper were tilted for 7.4 seconds, putting the structure on those stories in danger. The structure began to tilt significantly from its initial position after 8 seconds, and the hinge assembly is now in a dangerous scenario.

iii) Corralitos Earthquake

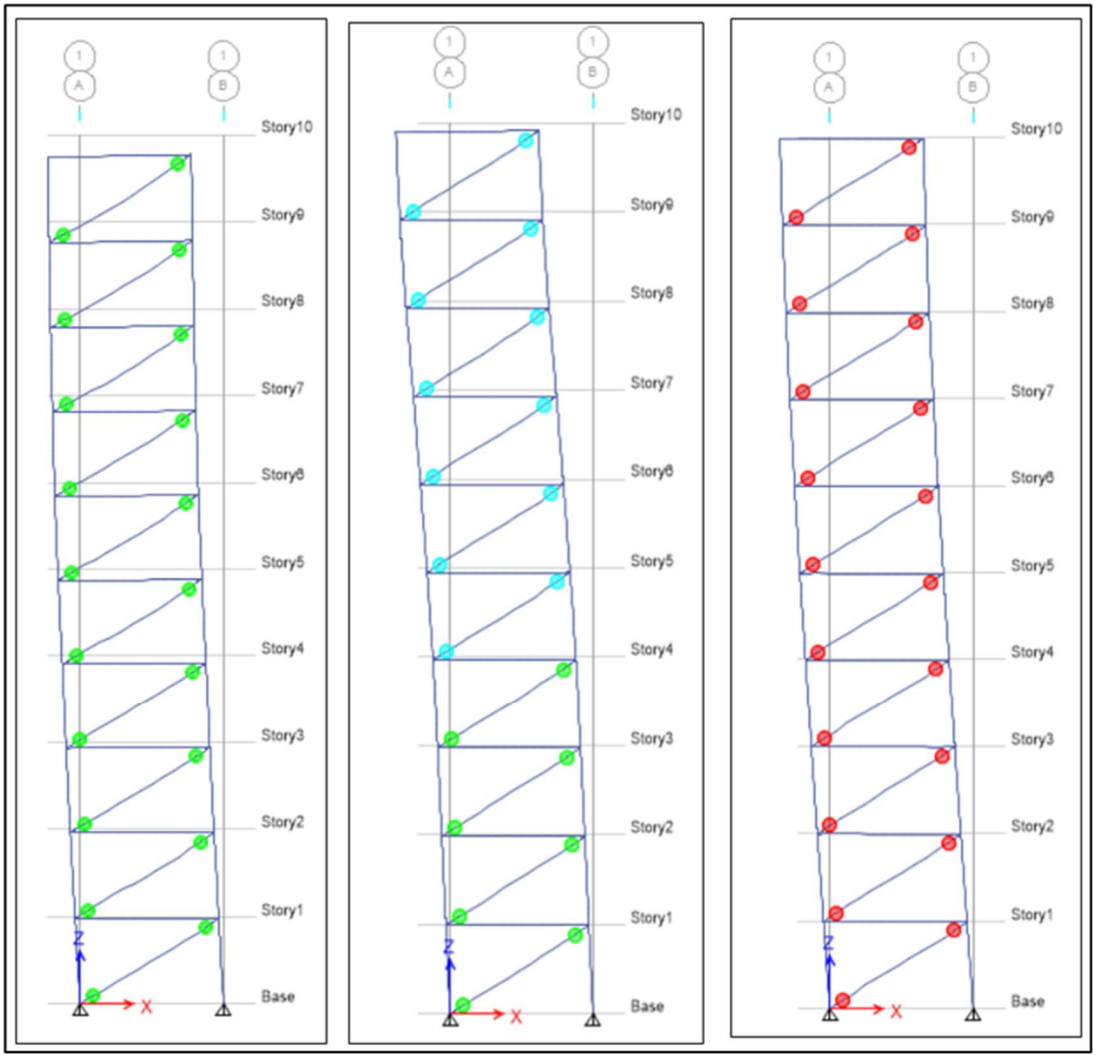

Fig. 14 Formation of hinges at 2.1sec, 3.5 sec and 15sec for Corralitos earthquake.

The formation of hinges for Corralitos earthquake for a 10-story structure is shown in fig. 14 above. To assess hinge development, the three time intervals are 2.1 seconds, 3.5 seconds, and 15 seconds. It is visible that the hinges begin to develop at 2.1 seconds, although they are quite safe and do not pose any hazard problems. The 10 story skyscraper's 4 levels are secure while the hinges were still inclined for 3.5 seconds, but the structure is likely in danger above those stories. The structure began to tilt significantly from its initial position after 4 seconds, and the hinge assembly is now in a dangerous scenario.

iv) Hollister - South & Pine Earthquake

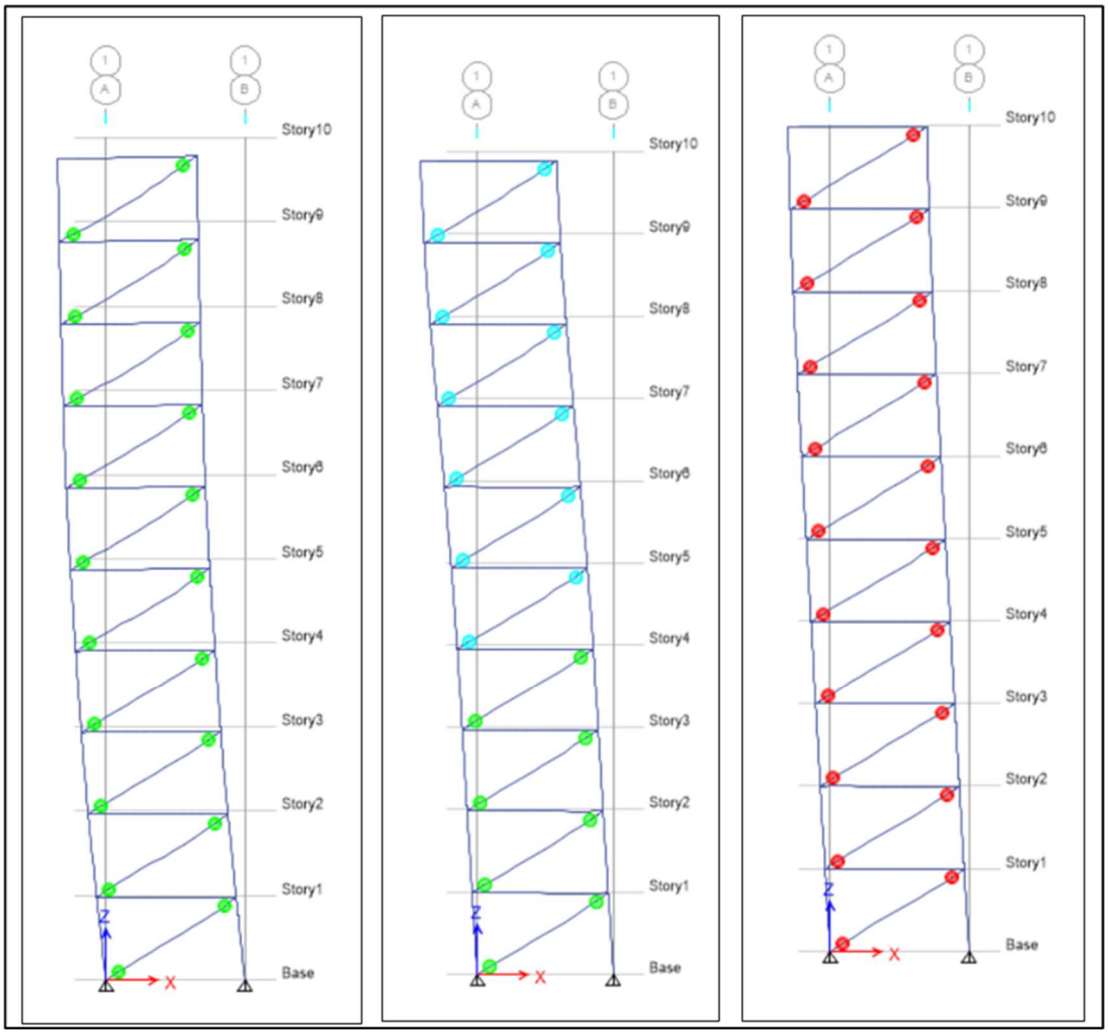

Fig. 15 Formation of hinges at 7sec, 10sec and 15sec for Hollister - South & Pine earthquake.

The formation of hinges for Hollister - South & Pine earthquake for a 10-story structure is shown in fig. 15 above. To assess hinge development, the three time intervals are 7 seconds, 10 seconds, and 15 seconds. It is visible that the hinges begin to develop at 7 seconds, although they are quite safe and do not pose any hazard problems. The 10 story skyscraper's 4 levels are secure while the hinges were still inclined for 10 seconds, but the structure is likely in danger above those stories. The structure began to tilt significantly from its initial position after 10 seconds, and the hinge assembly is now in a dangerous scenario.

v) Century City LACC North Earthquake

ISSN: 2096-3246
Volume 54, Issue 02, October, 2022

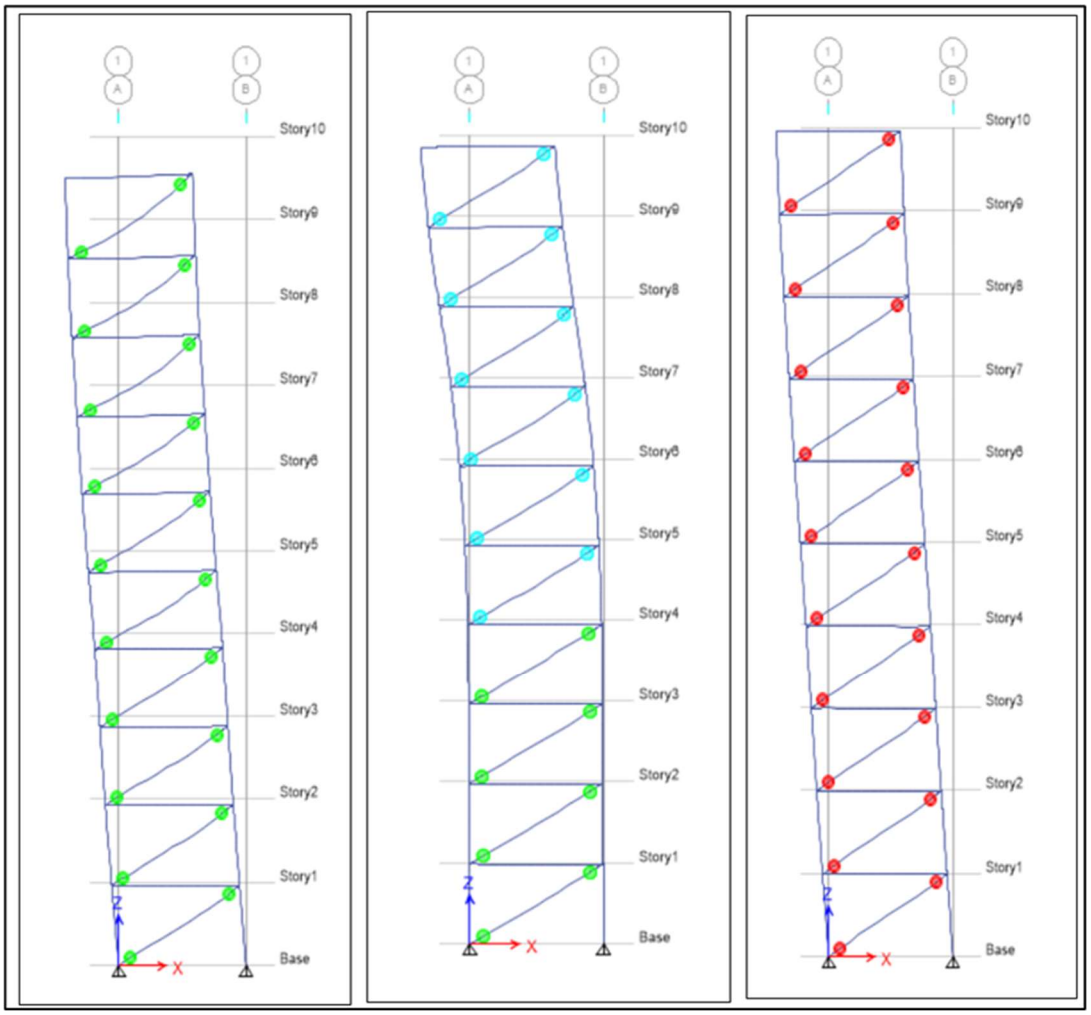

Fig. 16 Formation of hinges at 6sec, 8sec and 20 sec for Century City LACC North earthquake.

The formation of hinges for Century City LACC North earthquake for a 10-story structure is shown in fig. 16 above. To assess hinge development, the three time intervals are 6 seconds, 8 seconds, and 20 seconds. It is visible that the hinges begin to develop at 6 seconds, although they are quite safe and do not pose any hazard problems. The 10 story skyscraper's 4 levels are secure while the hinges were still inclined for 8 seconds, but the structure is likely in danger above those stories. The structure began to tilt significantly from its initial position after 8 seconds, and the hinge assembly is now in a dangerous scenario.

vi) Los Gatos - Lexington Dam Earthquake.

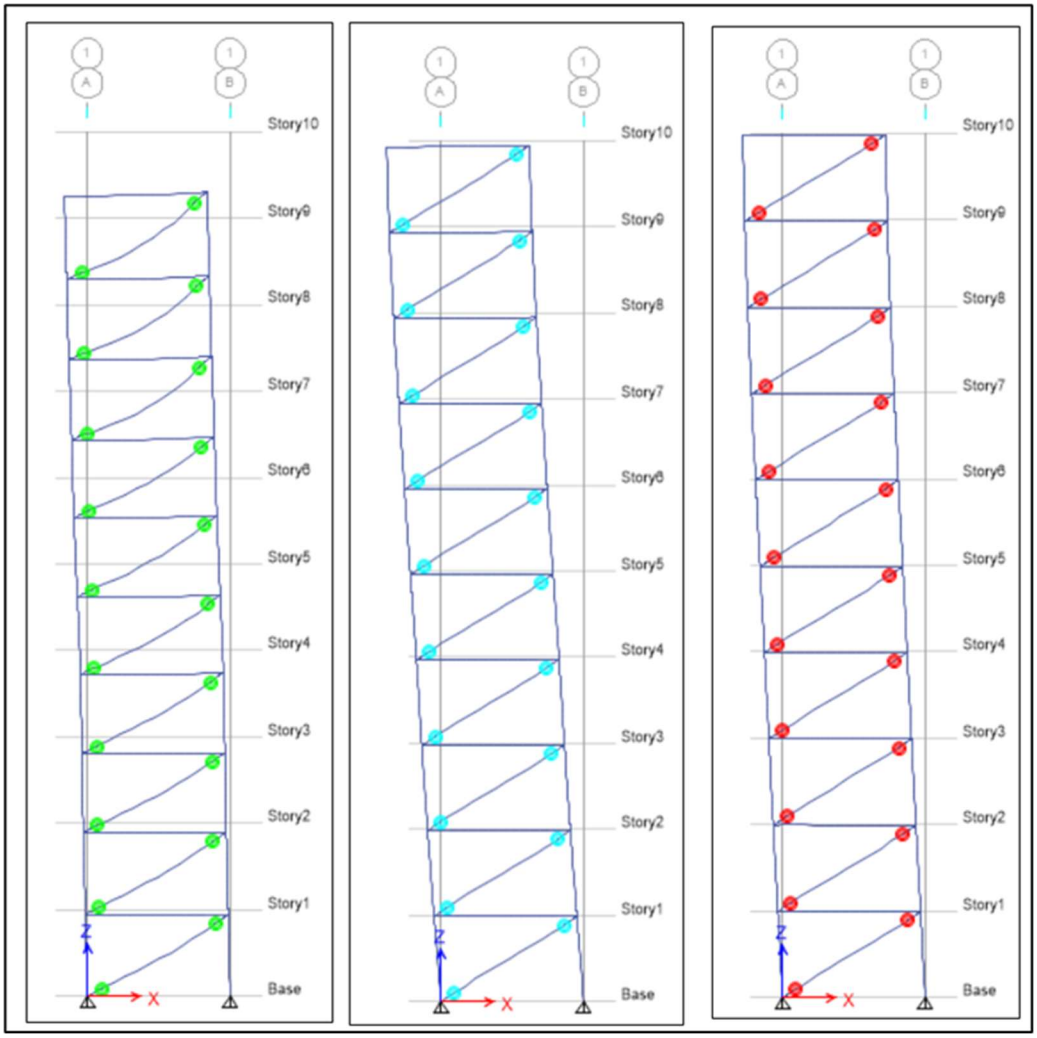

Fig. 17 Formation of hinges at 4.5 sec, 5.04 sec and 15sec for Los Gatos - Lexington Dam earthquake.
The formation of hinges for Los Gatos - Lexington Dam earthquake for a 10-story structure is shown in fig. 17 above. To assess hinge development, the three time intervals are 4.5 seconds, 5.04 seconds, and 15 seconds. It is visible that the hinges begin to develop at 4.5 seconds, although they are quite safe and do not pose any hazard problems. The hinges on the entire level of the 10-story skyscraper were tilted for 5.04 seconds, putting the structure on those stories in danger. The structure began to tilt significantly from its initial position after 6 seconds, and the hinge assembly is now in a dangerous scenario.

vii) Lucerne Valley Earthquake

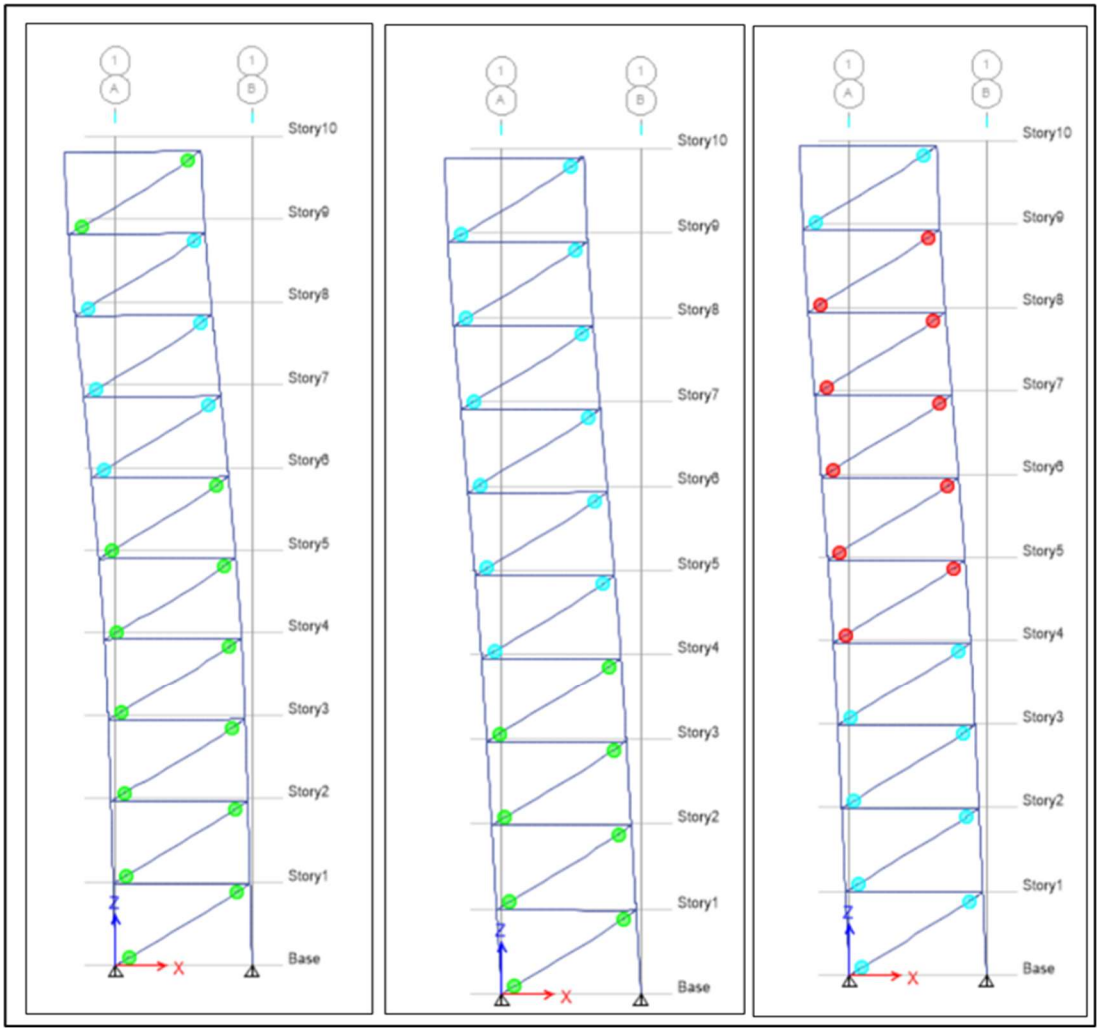

Fig. 18 Formation of hinges at 10.86sec, 12.5 sec and 20 sec for Lucerne Valley earthquake.

The formation of hinges for Lucerne Valley earthquake for a 10-story structure is shown in fig. 18 above. To assess hinge development, the three time intervals are 10.86 seconds, 12.5 seconds, and 20 seconds. It is visible that the hinges begin to develop at 10.86 seconds, although they are quite safe and do not pose any hazard problems. The 10 story skyscraper's 4 levels are secure while the hinges were still inclined for 12.5 seconds, but the structure is likely in danger above those stories. The structure began to tilt significantly from its initial position after 15 seconds, and the hinge assembly is now in a dangerous scenario.

6.3 Non Moment Resisting Braced Frame (NMRBF) with Dampers

6.3.1 Hinge status

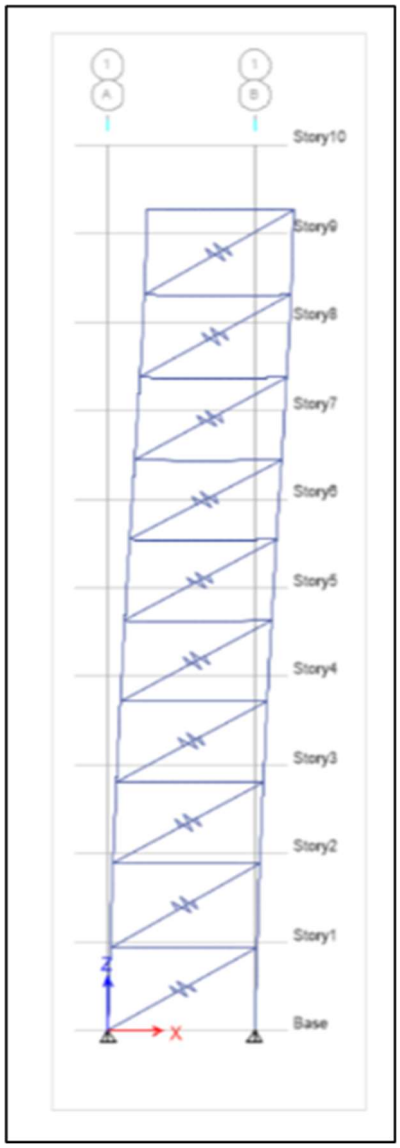

Fig. 19 No Formation of hinges for seven earthquakes

It is possible to deduce from the time history study that the NMRBF with dampers are now operating at an immediate operational level.

6.4 Hysteresis curve

6.4.1 Non Moment Resisting Braced Frame (NMRBF) with Dampers

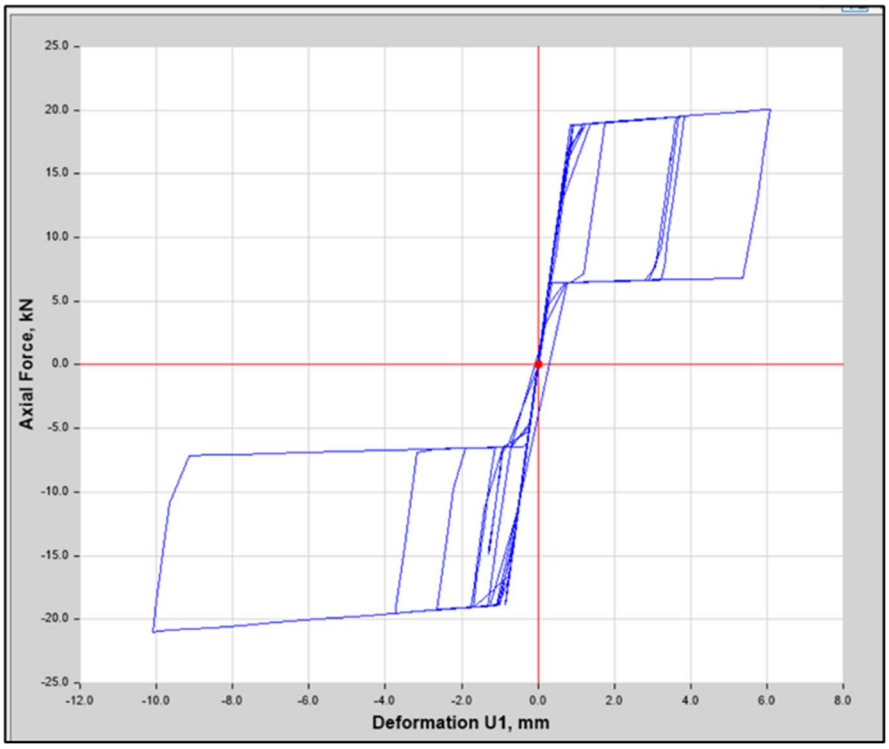

Fig. 6.40 Hysteretic curve of the RSFJ response under Altadena - Eaton Canyon Park.

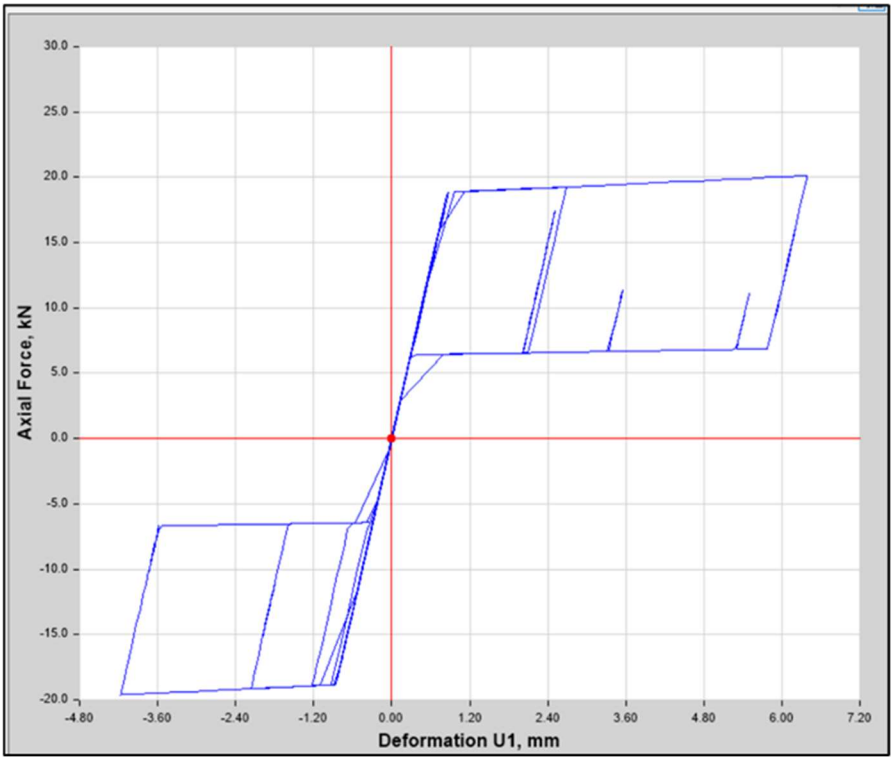

Fig. 6.41 Hysteretic curve of the RSFJ response under EL Centro Array earthquake.

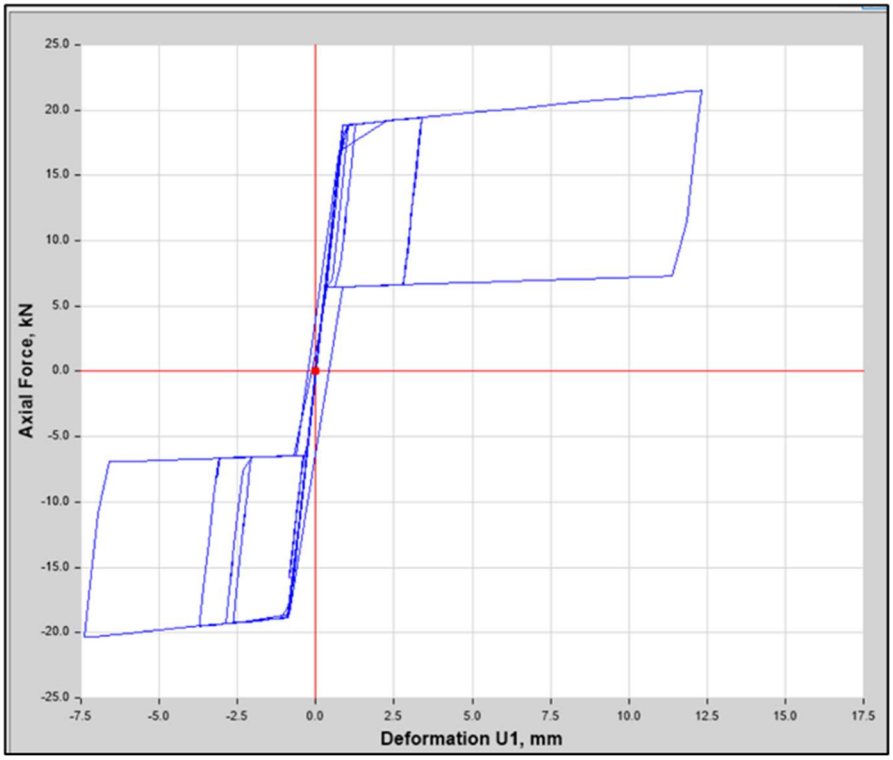

Fig. 20 Hysteretic curve of the RSFJ response under Corralitos earthquake.

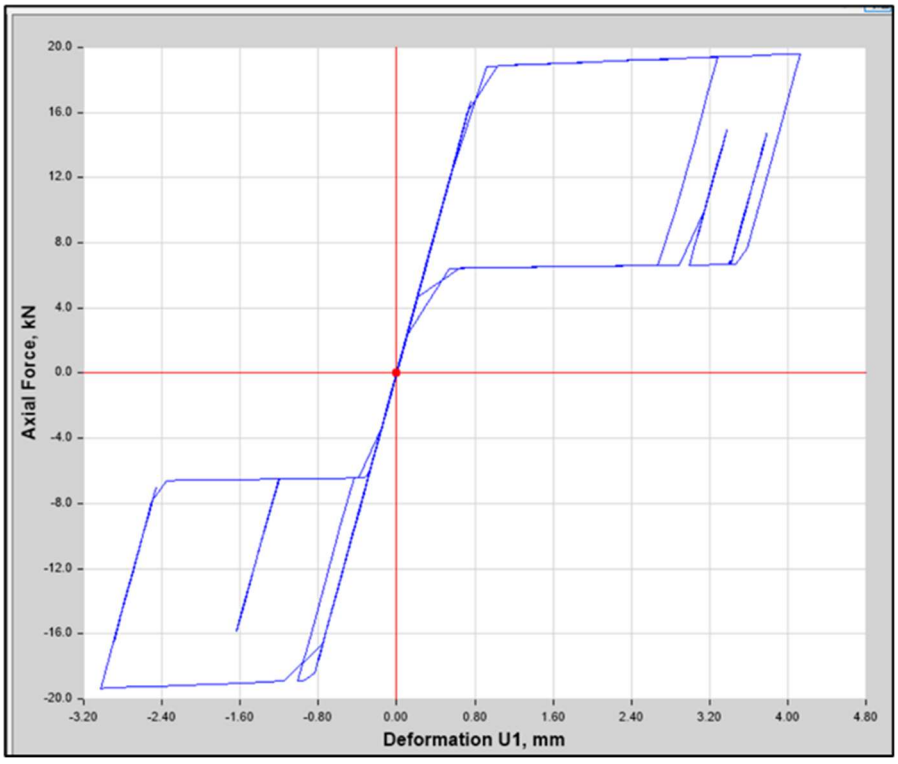

Fig. 21 Hysteretic curve of the RSFJ response under Hollister - South & Pine earthquake.

ISSN: 2096-3246
Volume 54, Issue 02, October, 2022

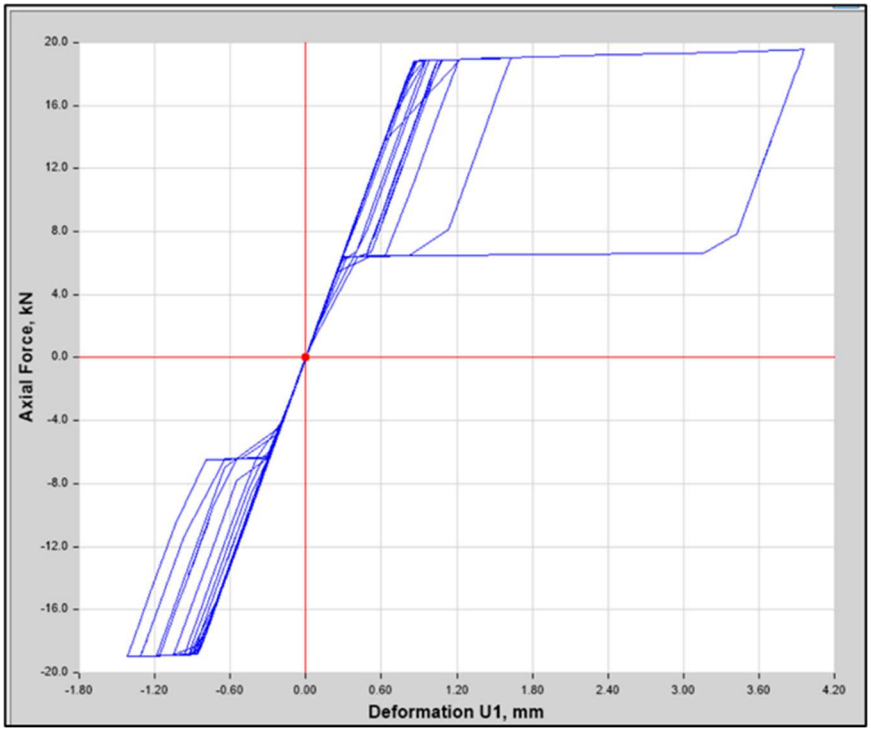

Fig. 22 Hysteretic curve of the RSFJ response under Century City LACC North earthquake.

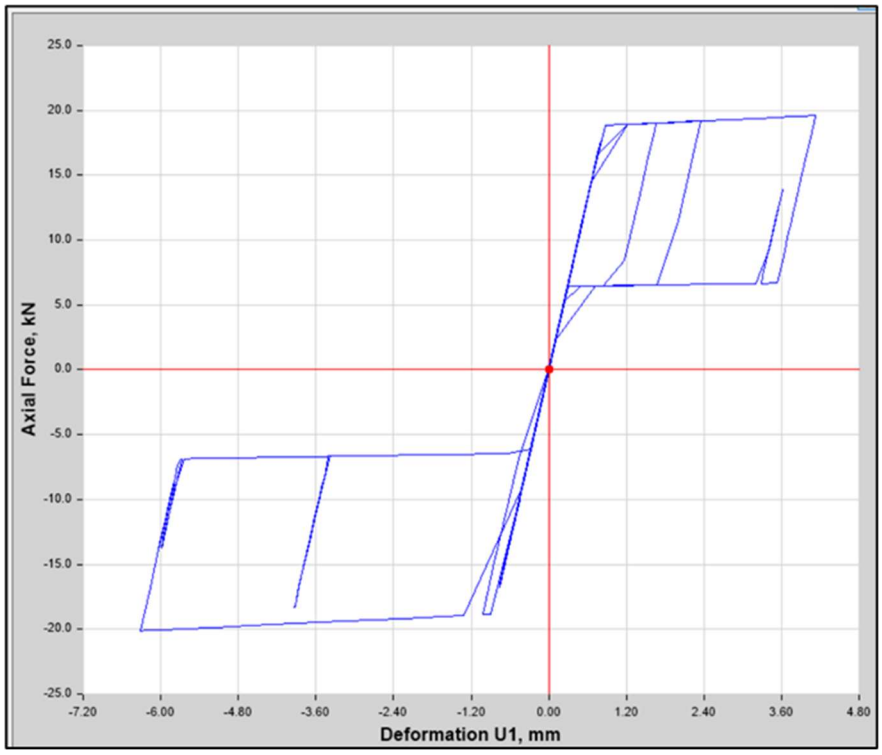

Fig. 23 Hysteretic curve of the RSFJ response under Lexington Dam earthquake.

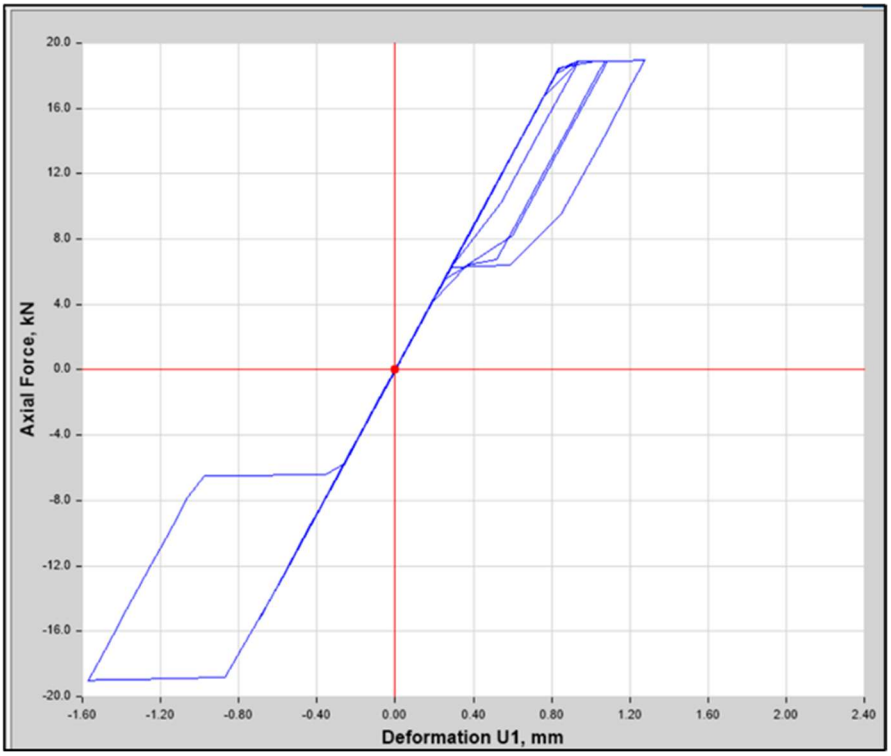

Fig. 24 Hysteretic curve of the RSFJ response under Lucerne Valley earthquake.

Figure 18 to 24 displays the load-deformation behavior of the top story RSFJ brace in seven of the MCE events. It can be seen that the RSFJ braces maintain their stable flag-shaped hysteresis. It should be noted that the residual displacements were zero for all of the cases (seven analyzed cases) which clearly demonstrates a fully self-centering behavior.

7. CONCLUSION

From the research study, it can be concluded that structure's response can be heavily reduced using resilient slip friction joint. Further from the pushover analysis, it can be concluded that the MRBF and NMRBF frames started tilting considerably from their original position and in the absence of resilient slip friction joint, they reaches collapse prevention threshold. Also for steel frames which are designed with IS 1893:2002 found to have significant performance like they are operational under MCE and posesses Elasticity under DBE. From the result analysis it can be concluded that to envisage the performance level of a building under a given earthquake, Pushover Analysis can be used as a well-designed tool. Also from time history analysis, it is analyzed that the percentage of reduction for the story displacement for MRBF and NMRBF with RSFJ.is 30% to 95%.

References

`[1] Qiu C, Liu J, Teng J, Li Z, Du X. Seismic performance evaluation of multi-story CBFs equipped with SMA-friction damping braces. Journal of Intelligent Material Systems and Structures.

2021;32(15):1725-1743. doi:10.1177/1045389X20987000.
[2] Francesca Barbagallo, Melina Bosco, Edoardo M. Marino, Pier Paolo Rossi, Seismic performance and cost comparative analysis of steel braced frames designed in the framework of EC8, Engineering Structures, Volume 240, 2021,112379,ISSN 0141-0296, https://doi.org/10.1016/j.engstruct.2021.112379.
[3] Zhu, L. and Zhao, C., 2020. Self-centering steel frame systems for seismic-resistant structures. Advances in Civil Engineering, 2020.
[4] Qiu, C. and Zhu, S., 2020. Enhance seismic performance of self-centering concentrically braced frames by using hybrid systems. Bulletin of Earthquake Engineering, 18(8), pp.3995-4015.
[5] Chi, P., Tian, W., Guo, T., Cao, D. and Dong, J., 2019. Parametric study on the seismic response of steel-framed buildings with self-centering tension-only braces. Advances in Civil Engineering, 2019.
[6] Sause, R., Ricles, J.M., Roke, D.A., Chancellor, N.B. and Gonner, N.P., 2010, July. Seismic performance of a self-centering rocking concentrically-braced frame. In Proceeding of the 9th US National and 10th Canadian conference on earthquake engineering (pp. 25-29).
[7] Kari, A., Ghassemieh, M. and Badarloo, B., 2019. Development and design of a new self-centering energy-dissipative brace for steel structures. Journal of Intelligent Material Systems and Structures, 30(6), pp.924-938.
[8] Casciati, S., 2019. SMA-based devices: insight across recent proposals toward civil engineering applications. Smart Structures and Systems, An International Journal, 24(1), pp.111-125.
[9] Hou, H., Li, H., Qiu, C. and Zhang, Y., 2018. Effect of hysteretic properties of SMA s on seismic behavior of self-centering concentrically braced frames. Structural Control and Health Monitoring, 25(3), p.e2110.
[10] Qiu, C.X. and Zhu, S., 2017. Performance-based seismic design of self-centering steel frames with SMA-based braces. Engineering Structures, 130, pp.67-82.
[11] Qiu, C., Li, H., Ji, K., Hou, H. and Tian, L., 2017. Performance-based plastic design approach for multi-story self-centering concentrically braced frames using SMA braces. Engineering Structures, 153, pp.628-638.
[12] Deylami, A. and Mahdavipour, M.A., 2016. Probabilistic seismic demand assessment of residual drift for Buckling-Restrained Braced Frames as a dual system. Structural Safety, 58, pp.31-39.
[13] Christopoulos, C., Tremblay, R., Kim, H.J. and Lacerte, M., 2008. Self-centering energy dissipative bracing system for the seismic resistance of structures: development and validation. Journal of structural engineering, 134(1), pp.96-107.